Preparation of Gold Nanoparticles Using Laser Ablation Technique: Influence of Wavelengths and Pulse Number

Maha M. Ibrahim , Faleh L. Mater and Sahar N. Rashid *

Department of Physics, College of Science, University of Tikrit, Salah al-Din, Iraq.

***Corresponding author E-mail:** sahar83@tu.edu.iq

https://doi.org/10.29072/basjs.20260114

ARTICLE INFO

Received: 29 August 2025

Accepted: 27 January 2026

Published: 30 April 2026

Keywords:

AuNPs, Colloids, Laser parameter, PLAL, SPR

ABSTRACT

The possibility of producing pure and impurity-free nanostructures makes laser ablation in liquids an interesting technique for producing nanostructure. This physical approach is easy, safe, economical, and fast compared to biological and chemical preparation techniques. In this work, the technique was applied to prepare gold nanoparticles using a pulsed Nd: YAG laser with constant energy and repetition rate. The wavelengths were varied, and three harmonics were used (1064, 532, and 355 nm). Ablation was performed using different pulse numbers (300, 400, and 500 pulses) for each harmonic, and deionized water was used as the liquid medium, resulting in a colloidal solution of a reddish-pink color that contained gold nanoparticles. The resulting nanoparticles were characterized both structurally and optically. In general, the average crystalline sizes of the resulting nanoparticles ranged between (9 - 15 nm), which appeared in different shapes as some samples were elliptical and some were spherical depending on the size and concentration resulting from changing the ablation parameters, where their average diameters ranged between (11- 46 nm). These parameters also affected the width and height of the absorption peak of the nanoparticles, which represents the surface plasmon resonance. It was thus found that (532 nm) is the best wavelength for preparation in this study.

1. Introduction

In the last few years, the process of laser-material interactions has gotten more attention in preparing metal colloids. Mafune et al. demonstrated the possibility of submerging the transition metals in liquid media and then targeting it using an operation for laser ablation. Such a procedure can produce metal colloidal' without contaminating ions [1]. In the 1990s, the ablation of metals in a liquid (as a solution) using the pulsed laser technique had appeared. Such techniques contain essential features based on their relative straightforwardness since they rely on irradiating a solid target with millijoule lasers in a liquid medium [2]. When the three dimensions of the particles are on the nanometer scale, these particles are called nanoparticles (NPs), also called quantum dots, which are extremely small crystals that behave as individual atoms whose properties can be controlled [3, 4]. The NPs' important properties, such as chemical, electronic, mechanical, and optical properties, are different from the material of microscopic or the biggest. In general, there are two types of approaches to preparing nonmaterial's: the first is a top-down approach, which includes several methods based on the principle of removing nanoparticles from solid materials [5], and the second is a bottom-up approach, which includes many methods that usually begin with the atoms that combine to generate nanostructures [6]. Such nonmetric particles are attractive for electronics, catalysis, and medicine; increased requests for NPs have come due to their compatibility with various applications due to their properties, such as geometric shape, composition, size, and arrangement [7, 8]. Characterizing the surface composition of NPs and their precise control, in addition to their crystalline structures are very important in all cases due to their high surface reactivity and multifunctional capabilities [3]. Nanoparticles of Gold (AuNPs) have obtained wide acceptance and great interest among all the other various NPs widely available among researchers due to their wide range of applications, such as in sensors [9]. Much of the scientific research has focused on the methods of the synthesis of NPs based on the reduction of gold compound precursors such as AuCl [10, 11]. During the past ten years, various AuNPs with different shapes were investigated, noting that the surface plasmon resonance (SPR) of AuNPs has been designed by tuning and controlling their sizes. In particular, the anisotropic properties of AuNPs are most attractive due to their unique optical, magnetic, electrical, and plasmonic properties, as well as a variety of modern forms and applications of AuNPs are influential in the optical, catalytic, and biomedical fields [12]. Some of the intelligible advantages of applying AuNPs are when the diameter is very tinny on the order of or less than (5 nm), they can used as a catalyst, transform airborne pollutants into innocuous molecules [13], used AuNPs in therapeutic medicines and treating cancerous tumors in the body and the ability of AuNPs to

convert specific wavelengths of light into heat [14]. Due to their various electronic and optical properties, AuNPs have been used in cell imaging using different techniques [6]. AuNPs play an important role in electrochemical sensors due to their chemical stability and excellent electrical conductivity [15], also, the surface of AuNPs can contribute to detection and biometrics by selectively bounding to biomolecules by appropriate functionalization [16, 17]. AuNPs have shown amazing applications for diagnostic, as well as therapeutic utilize, such as biosensor applications, accurate drug delivery of nano-vehicles to diseased tissues, and tumor-targeting capability for cancer therapy [12]. Laser irradiation at a wavelength close to SPR wavelength can fragment NPs and aggregates when applied to colloidal solution [13], and additional laser irradiation had a more significant effect on the size distribution of NPs in water compared to glucose solution. Initial NPs are more stable in glucose solution and have a narrower size distribution due to the stabilization impact of glucose solution [18]. Figure 1 shows applications of AuNPs in various fields [19]. NPs can produce via ablation from a solid target utilizing laser short-pulses [20]. Laser ablation uniquely resolves the cytotoxic effects reported for nanoparticles resulting from chemical synthesis, where a big advantage of laser-generated NPs is the exclusion of byproducts or toxic substances since chemical precursors are not needed [21, 22]. When the laser energy is used on a solid or liquid surface, the material is heated when the target absorbs the laser's energy, causing evaporation because of the high temperature and, as a result, turning the material into plasma. The ablation rate (the number of particles removed using a laser pulse) depends on the laser energy, its inflow in the material, and the material optical characteristics [23]. One of the methods used to produce and manufacture colloidal NPs in several types of solutions is the laser ablation method [24]. The method of laser fragmentation in liquids (LFL) is considered to be fine particle dispersions [20]. One of the most significant benefits inherent in this process is the decrease of byproducts generated in the laser ablation process, as only the basic fluid and the target material are required. In addition, it allows the synthesis of alloy NPs, noting that these NPs are in high demand in catalysis, nanomedicine, or other manufacturing [8, 25]. Figure 2 shows the sketch of the main experimental features of pulsed laser ablation in liquid (PLAL) [26]. Deionized water is the most commonly used in PLAL in the studies of NPs synthesis, where phase, size, surface chemistry, morphology, and composition are investigated [27, 28]. Studies have proven the stability of AuNPs prepared by the PLAL technique by characterizing its solution absorbance and morphology [21]. This technique proves the possibility of obtaining AuNPs without functionalization, and offer size distributions that defined by the parameters of technique, which enables control over the AuNPs diameters, which is crucial for their usage in

colorimetric sensing [27]. Recently, the PLAL technique has been used to produce AuNPs with narrow size distribution using surfactants to quench the growth. The advantages of laser-generated AuNPs include high purity with unique surface properties [29]. The parameters of the laser ablation play a fundamental role in the properties of the resulting NPs, most notably the wavelength, number of pulses, and pulse energy [30-37]. There are several studies regarding the effect of laser parameters on the properties of the resulting AuNPs. Hisham et al. [38] studied the laser beam energy on the prepared AuNPs and found that with increasing energy the size of the NPs decreases until they reach their critical size at which the particles become insensitive to laser energy. When the energy exceeds this size, the NPs begin to clump together again and their size increases. The wavelength also affects the size and quantity of the NPs. As LaHaye et al. [39] have shown, the ablation threshold is lower when shorter wavelengths are used, this has been confirmed by studies on the laser ablation of various NPs [32]. Changing the laser wavelength plays a crucial role in pulsed laser ablation, as it affects the pulse energy and consequently the ablation rate and the quality of the treated material. This is because it influences the material's absorption properties, which in turn affects the level and quality of the resulting ablation. Shorter wavelengths lead to more effective ablation compared to longer wavelengths. This is due to the higher photon energy, which increases the material's absorption coefficient as the laser wavelength decreases. This suggests that using shorter wavelengths may result in more effective ablation [40].

Figure 1. AuNPs applications **[19]**

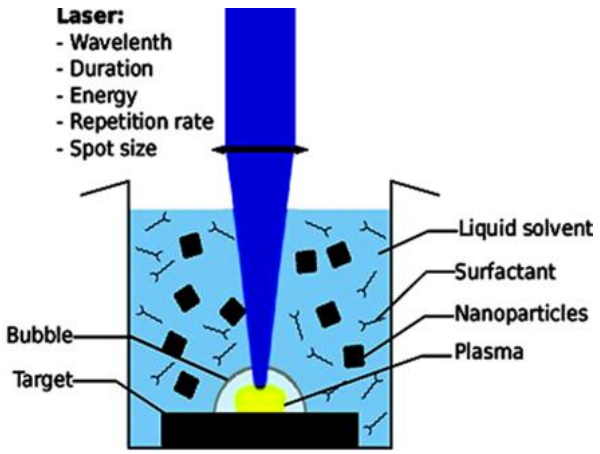

Figure 2. PLAL mechanism **[27]**

This work aims to synthesize AuNPs using the ablation technique with a pulsed Nd: YAG laser in deionized water. The used methodology includes the prepared of AuNPs using PLAL at different wavelengths and pulse numbers and then the structural and optical characterization of the resulting NPs to reach the best parameters for preparation as a preliminary study towards

various future investigations. The novelty of this work lies in conducting a systematic study to evaluate the effect of multiple laser wavelengths and pulse counts and to determine the optimal parameters for controlling the properties of gold nanoparticles free from impurities and chemicals on their surface, enabling their use in fields that require high-purity particles for medical or environmental applications.

2. Materials and Methods

2.1. Materials

The materials used in this work are simply a piece of high purity gold and deionized water as a liquid medium for the ablation process.

2.2. Methods

The practical part of this study was conducted in the Optics and Laser Laboratory at the College of Science at Tikrit University. Colloidal solutions containing AuNPs were prepared using the ablation technique with a pulsed Q-switch Nd: YAG laser from Beijing Sincoheren S&T Development Co., Ltd – China, with energy (100 mJ) and a repetition rate (3 Hz) using three wavelengths (1064, 532, and 355 nm) and changing the number of pulses (300, 400, and 500 pulses) for each wavelength, these pulse numbers were chosen based on experiments conducted under working conditions, where reaching this number of pulses caused a color change in the resulting colloidal solutions, which serves as evidence of NSs formation in these solutions. This work focused on the effect of wavelength and pulse number using a constant energy (100 mJ), but it's important to note that the pulse energy loss occurs during the transition to second and third harmonics. This loss is a gradual decrease due to the light passing through nonlinear crystals to double the frequency. The loss is often in the form of heat. However, this loss is compensated for by the fact that the photon energy will be high during the transition to second and third harmonics as a result of the frequency doubling.

The pure gold slice was placed inside (5 ml) of deionized water, and the laser source was at a height of (15 cm) above the sample, while the liquid level up the target sample was (5 mm). After that, the optical and structural properties of the prepared solutions were determined using the X-ray Diffraction (XRD) technique, Field-Emission Scanning Electron Microscope (FESEM), the Energy Dispersive X-ray (EDX) microanalysis, and UV-visible (UV-Vis) spectrophotometer. The drop casting method was used to prepare the samples as thin films to determine their structural and morphological properties using XRD and FESEM techniques,

respectively, where the prepared nano-solution is distilled using a pipette on a glass slide and placed on the hotplate stirrer to be at a temperature (~ 40 ºC) to dry it [23].

3. Results and Discussion

3.1. Optical Properties (UV-Vis Analysis)

The colloidal solutions resulting from the preparation process appeared reddish-pink in color for all the prepared samples because they contained AuNPs. It was noted that the color intensity increases with the pulse number increase, which indicates NPs concentration increase formed in the colloidal solution, as in Figure 3, which generally shows that the preparation at the wave-length (532 nm) produces a redder solution compared to the other two wavelengths.

The first measurements of the prepared solutions were by measuring the absorbance spectrum using the UV-Vis technique. The absorption spectrum in Figure 4 for all prepared samples shows the appearance of a peak indicating SPR of the AuNPs around the wavelength (527 nm), resulting from the coordination of the collective oscillation of the surface electrons of the material with the frequency of photons of light falling on them, which caused the color of the solution containing the nanoparticles to change. It was observed that increasing the number of pulses from (300 pulse) to (400 pulse) for all wavelengths used led to an increase in absorption intensity, as evidenced by an increase in peak height and width. This resulted from an increase in the concentration of NPs, since the number of NPs ablated within the liquid increased with the number of pulses. However, with an increase in the number of pulses to (500 pulse), the absorption intensity decreased. This is attributed to the accumulation of ablated NPs on top of the target sample, which causes some obstruction to the laser pulses reaching the target for further ablation. In other words, this accumulation reduced the ablation efficiency [41]. A slight red shift in the SPR peaks of the prepared NPs at the three wavelengths can be observed with the increasing number of pulses due to their increasing sizes, indicating a change in the energy level of the material [42, 43]. The resulting difference in the broadness of the peaks at different concentrations of the prepared NPs at the different preparation parameters is due to the difference in their size distributions. When comparing this spectrum for the samples prepared with the highest number of pulses and for the three wavelengths, it is noted that the highest absorption intensity belongs to the sample prepared with the wavelength (532 nm), which is consistent with what was obtained in the colors of the colloidal solutions, which showed that the most concentrated solutions are those prepared with this wavelength, as in Figure 4.d. In other words, from this figure, it is clear that the wavelength (532 nm) led to an increase in the concentration of the prepared AuNPs and the regularity of their size distribution by observing

the broadness and height of the absorption peak, in addition to increasing the energy levels of these particles as a result of the peak blue-shift [44-46]

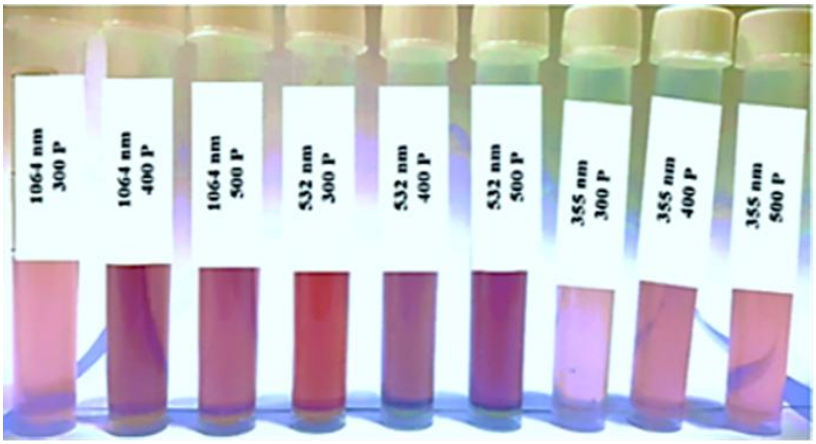

Figure 3. Prepared AuNPs colloidal solution colors

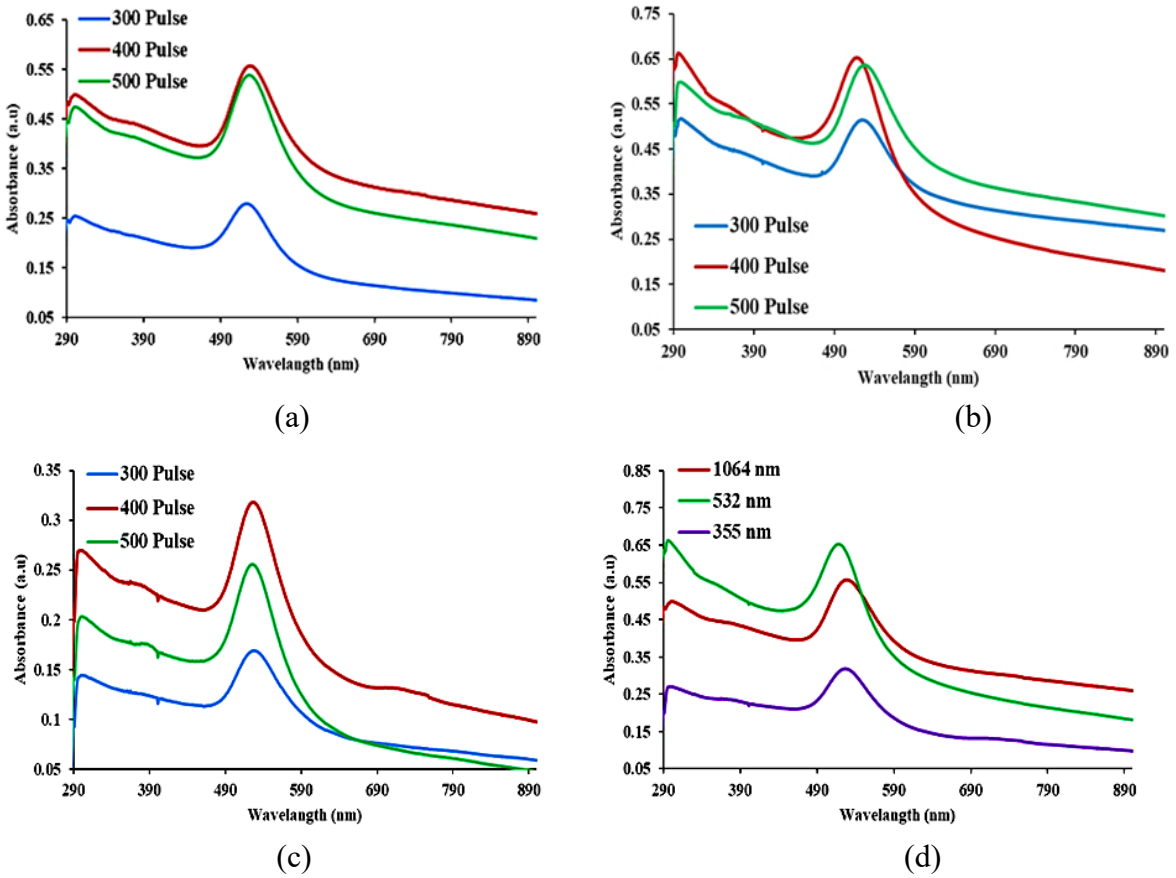

Figure 4. Absorption spectrum of AuNPs prepared with different pulse numbers at: (a) 1064 nm, (b) 532 nm, and (c) 355 nm, (d) Comparison of the absorption spectrum when preparing with the highest number of pulses at the three wavelengths

3.2. Structural Properties Analysis

The crystallinity of prepared AuNPs was analyzed by the XRD technique, and corresponding XRD patterns were shown in Figure 5.a,b,c that the AuNPs exhibited four distinct peaks corresponding to the standard JCPDS card no. (00-004-0784) [48] of face center cubic (fcc) lattice with preferential directions whose levels are represented by Miller indices (111), (200), (220), and (311), it has been shown that the dominant trend is at (111) for all prepared NPs, where the highest intensity of diffractive X-rays; is recorded. The crystalline sizes of the synthesized NPs (D) were calculated using the Scherer equation [20] (Equation 1) by analyzing the results of the XRD test', by calculating the full width of half maximum (FWHM = β) of the peaks belonging to the diffraction angles (2θ) were obtained for all samples, noting that the wavelength of the used X-rays is (λ = 1.54 Å):

$$D = \frac{0.9\lambda}{\beta \cos\theta} \quad \textbf{\textit{Eq}.1}$$

It was found that the crystalline average sizes of NPs for the prepared samples are small, ranging between (9 – 15 nm). Their values were as follows (10.7, 10.5, and 14.8 nm) for pulses (300, 400, and 500) respectively when preparing with wavelength (1064 nm), and (11.5, 10.4, and 9.8 nm) for pulses (300, 400, and 500) respectively when preparing with wavelength (532 nm), and (9.9, 9.4, and 10 nm) for pulses (300, 400, and 500) respectively when preparing with wavelength (355 nm). XRD data are shown in Table 1. The increase in the crystalline average size of incoming NPs at the highest number of pulses of the two wavelengths (1064 and 355 nm) is due to the occurrence of accumulation and aggregation of the resulting NPs as a result of increasing concentration. It is obvious that changing the wavelength while maintaining constant ablation energy has a significant impact on the pulse energy; switching to a shorter wavelength produces less pulse energy, which affects ablation efficiency [40]. The effect of using the wavelength (532 nm) in the preparation is noted, as increasing the pulse number led to a regular decrease in the crystalline size of the NPs, which indicates that this wavelength is the most appropriate in preparing AuNPs under the current working conditions comparatively with the other two wavelengths as shown in Fig 5.d, this was proven by the results of the analysis of the optical properties regarding the use of this wavelength. In this figure, all crystallographic orientations and properties were analyzed relative to the (111) plane as it exhibited the primary diffraction peak, ensuring a consistent baseline for comparison across all

samples. The diagram in this figure shows the irregularity in the increase or decrease in the crystalline size of the synthesized NPs using the first and third harmonics (1064 and 355 nm) when increasing the number of laser pulses, with a clear increase in the average size observed at the highest number of pulses, specifically using the wavelength (1064 nm), while it became clear that the second harmonic (532 nm) is the most suitable for controlling the average size by regularly obtaining smaller size as the number of pulses increases. Although the same number of pulses are used for all wavelengths, the pulse energy varies according to the wavelength, being lower as the wavelength decreases, as we mentioned earlier, and this is a crucial factor in the ablation process.

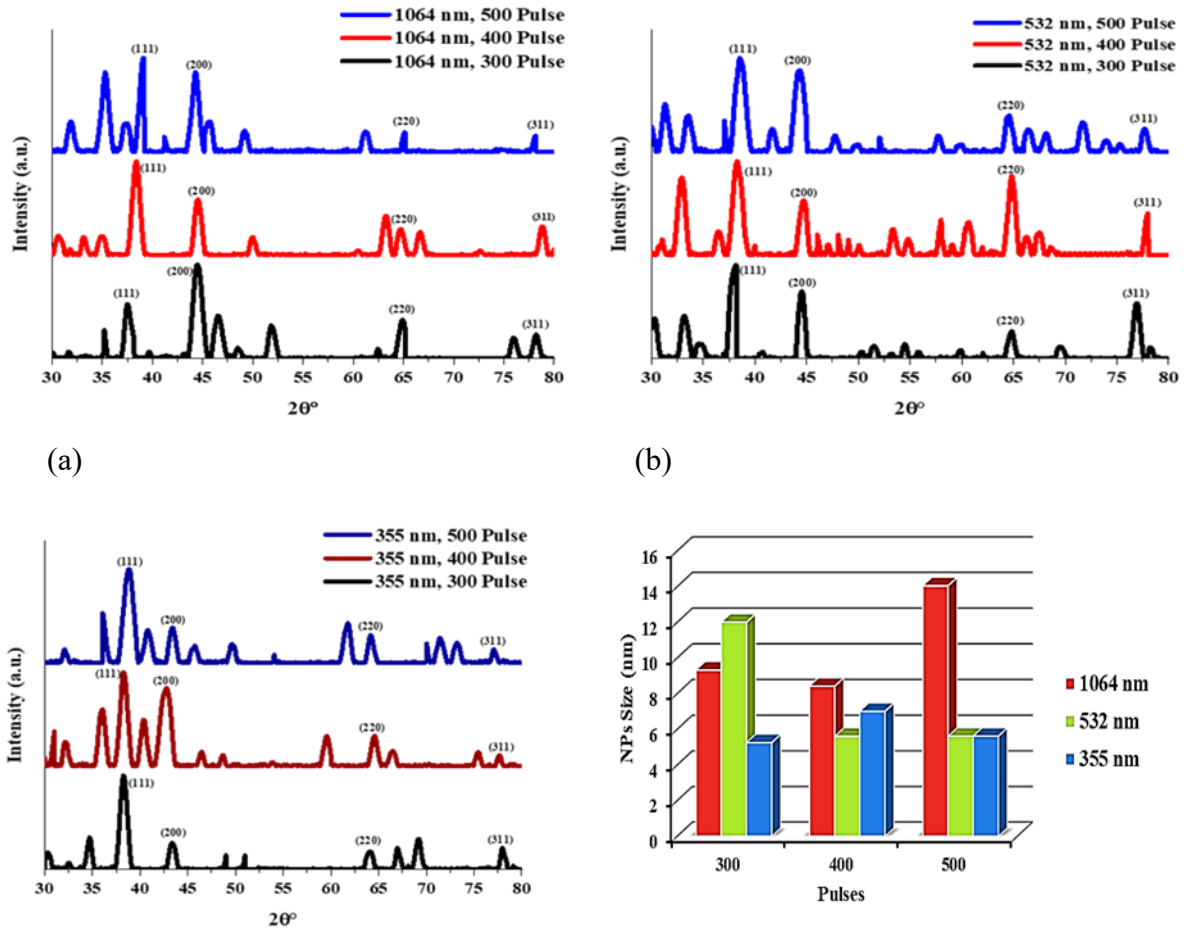

Figure 5. XRD patterns of AuNPs prepared with different pulse numbers: (a) at 1064 nm, (b) at 532 nm, (c) at 355 nm, (d) Comparison of crystalline sizes for all synthesized NPs

Table 1. XRD data of prepared AuNPs

λ (nm)	Pulse no.	2θ (deg)	hkl	β (deg)	d (nm)	D (nm)
1064	300	37.5	111	0.9	0.2395	9.3180
		44.5	200	1	0.2033	8.5800
		64.9	220	0.7	0.1435	13.443
		78	311	0.9	0.1223	11.353
1064	400	38.5	111	1	0.2335	8.4114
		44.5	200	0.9	0.2033	9.5334
		64.5	220	1	0.1442	9.3897
		78.5	311	0.7	0.1217	14.649
1064	500	39	111	0.6	0.2306	14.040
		44	200	1.5	0.2055	5.7099
		65	220	0.5	0.1433	18.831
		78	311	0.5	0.1223	20.436
532	300	38	111	0.7	0.2365	11.998
		44.5	200	0.9	0.2033	9.5334
		64	220	0.7	0.1453	13.377
		77	311	0.9	0.1236	11.274
532	400	38.2	111	1.5	0.2353	5.6025
		44.5	200	0.9	0.2033	9.5334
		64.8	220	1	0.1437	9.4053
		78	311	0.6	0.1223	17.030
532	500	38.5	111	1.5	0.2335	5.6076
		44	200	1.5	0.2055	5.7099
		64.5	220	0.7	0.1442	13.413
		77.5	311	0.7	0.1230	14.546
355	300	38	111	1.6	0.2365	5.2492
		43.5	200	0.9	0.2077	9.4998
		64	220	0.9	0.1453	10.404
		77.8	311	0.7	0.1226	14.577
355	400	38.2	111	1.2	0.2353	7.0031
		42.9	200	1.5	0.2105	5.6881
		64.5	220	0.9	0.1442	10.433
		77.5	311	0.7	0.1230	14.546
355	500	38.8	111	1.5	0.2318	5.6128
		43.3	200	0.9	0.2087	9.4932
		64	220	0.9	0.1453	10.404
		76	311	0.7	0.1250	14.396

The results of the analysis of the FESEM technique regarding the surface morphology of the prepared gold NPs are shown in Figs. 6 – 14, which show images of the AuNPs at two scales (100 and 500 nm). These images showed, in general, the resulting NSs composed in with different shapes depending on the laser parameters, specifically the wavelengths and their effect on the pulse energy, as well as the effect of the number of pulses, as some samples were elliptical and some were spherical, and this depends on the preparation conditions and the resulting concentrations. The results showed that the NSs produced by using the wavelength (1064 nm) at the three numbers of pulses used were elliptical in shape, tending to form larger aggregates that tend towards a cubic shape, and their diameters ranged between (11 - 34 nm). As for the prepared NPs at a wavelength of (532 nm), their diameters ranged between (26-32 nm) and they were spherical in shape and also tended to form aggregates. The same was true for the prepared NPs at a wavelength of (355 nm), while their average diameters ranged between (24-46 nm). The formation of aggregates and clumps is due to the high concentration of formed NPs in their colloidal solutions due to the increase in the laser energy density rate, which consequently led to an increase in the diameter average of NPs. When the laser strikes the target, it generates a high-temperature, high-pressure plasma. As this plasma cools rapidly (especially in liquids), the vaporized atoms begin to clump together, forming tiny nuclei that move within a bubble created by the laser. These nuclei then collide continuously, merging to form clusters. The high surface energy of the NPs makes them unstable, causing them to clump together to reduce this energy and achieve a more stable state. There is no protective coating to prevent the formation of these clusters, particularly with PLAL, which is clean and does not use chemicals that could inhibit cluster formation [48], led to a size disparity and, thus, a difference and irregularity in the size distribution. Shorter wavelengths possess high photon energy, leading to the vaporization of a larger quantity of matter. This increases the vapor concentration in the reaction region, promoting the agglomeration, clustering, and rapid growth of particles before they stabilize. The differences in the average of diameters of the resulting NPs are attributed to the wavelength effects used in ablation, as the wavelength directly controls the mechanism of energy absorption and the size of the resulting particles according to the absorption efficiency, the ablation threshold and the plasma interaction. At long wavelengths, the plasma blocks the laser from the target, which reduces the fragmentation efficiency and increases the growth of particles by fusion [49]. Based on the FESEM results, it is clear that the NPs synthesized at wavelength (532 nm) are the best as they have spherical shapes and smaller diameters. Spherical AuNPs have several useful properties, such as optoelectronic capabilities related to shape and size [50], high biocompatibility, low toxicity, and high surface-to-volume ratio [51].

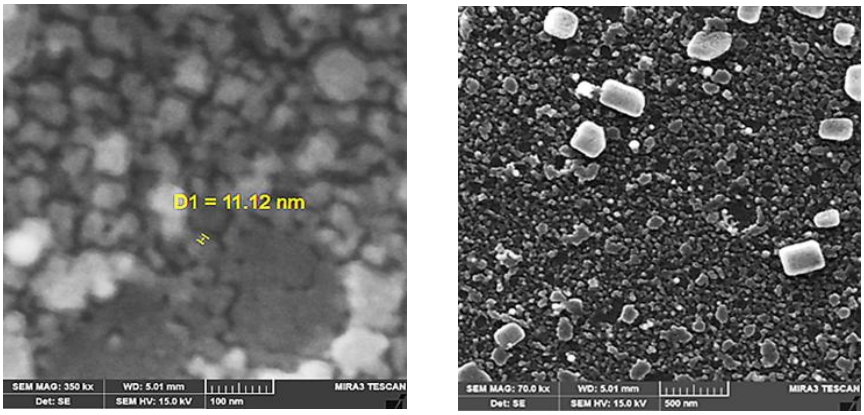

(a) (b)

Figure 6. FESEM images of AuNPs synthesized at 1064 nm, 300 pulse with the scales: (a) 100 nm, (b) 500 nm

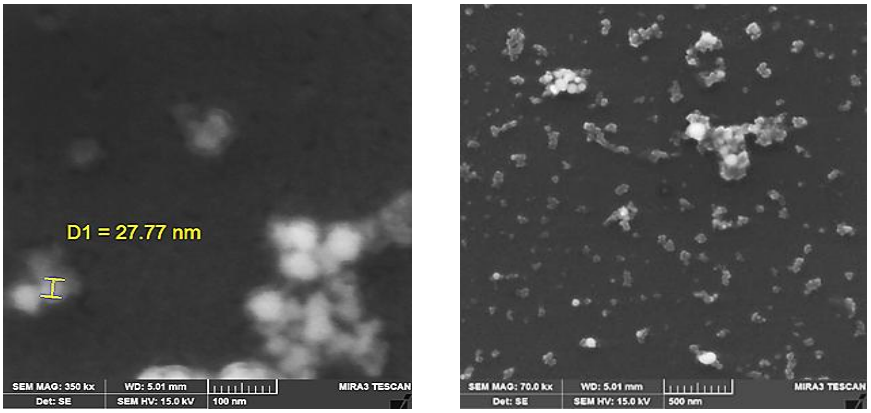

(a) (b)

Figure 7. FESEM images of AuNPs synthesized at 1064 nm, 400 pulse with the scales: (a) 100 nm, (b) 500 nm

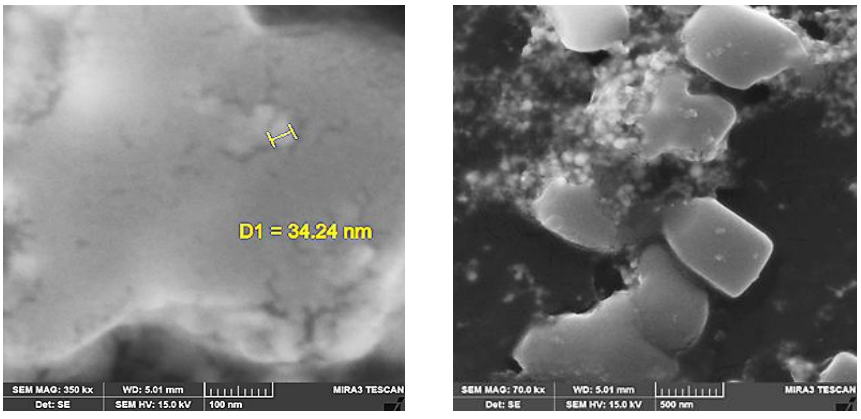

(a) (b)

Figure 8. FESEM images of AuNPs synthesized at 1064 nm, 500 pulse with the scales: (a) 100 nm, (b) 500 nm

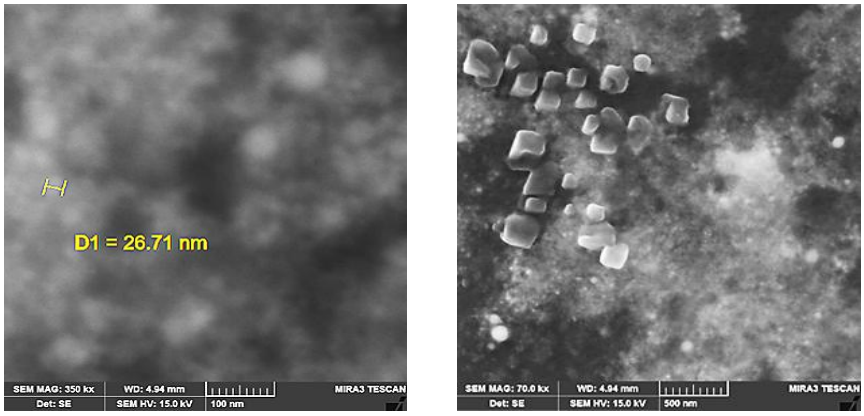

(a) (b)

Figure 9. FESEM images of AuNPs synthesized at 532 nm, 300 pulse with the scales: (a) 100 nm, (b) 500 nm

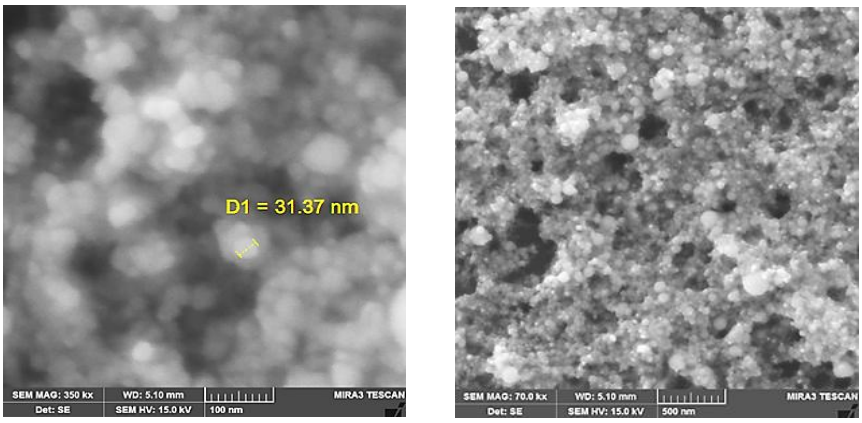

(a) (b)

Figure 10. FESEM images of AuNPs synthesized at 532 nm, 400 pulse with the scales: (a) 100 nm, (b) 500 nm

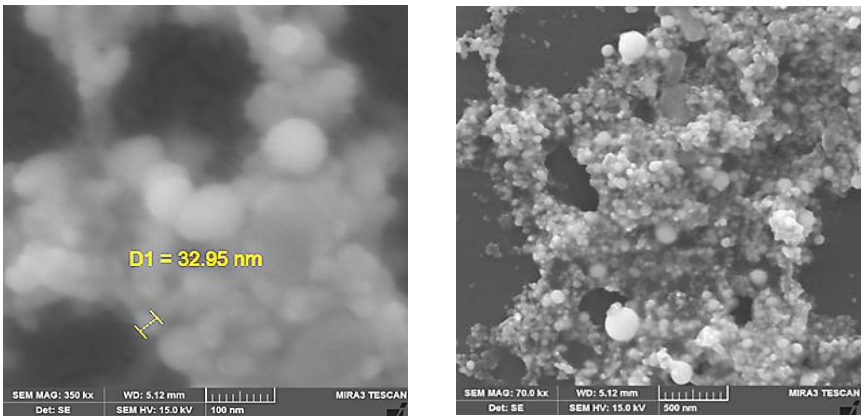

(a) (b)

Figure 11. FESEM images of AuNPs synthesized at 532 nm, 500 pulse with the scales: (a) 100 nm, (b) 500 nm

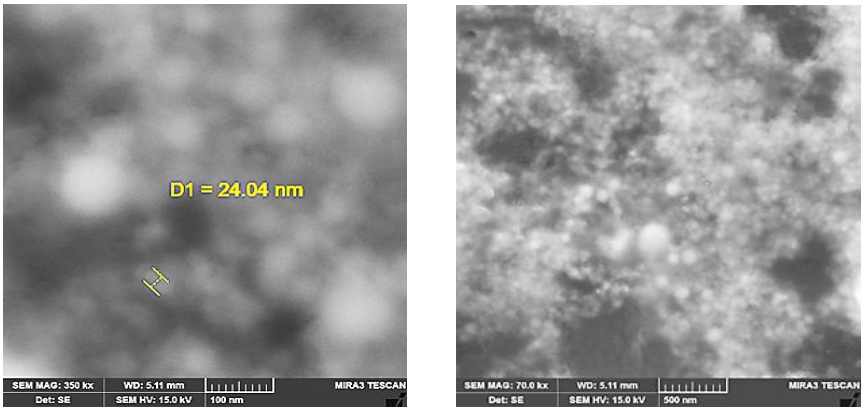

(a) (b)

Figure 12. FESEM images of AuNPs synthesized at 355 nm, 300 pulse with the scales: (a) 100 nm, (b) 500 nm

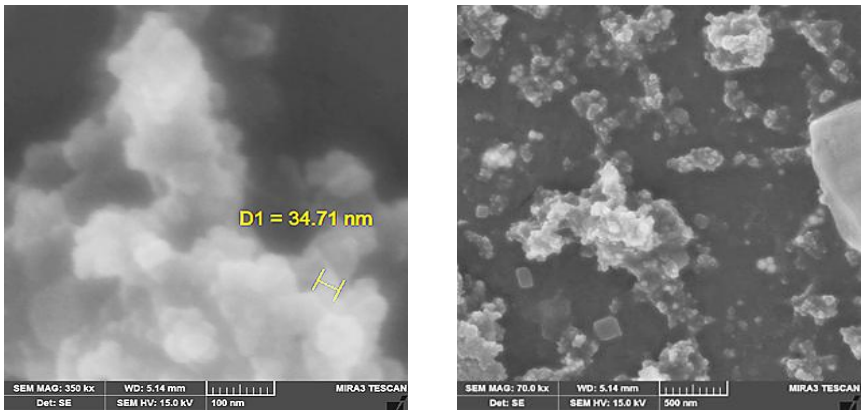

(a) (b)

Figure 13. FESEM images of AuNPs synthesized at 355 nm, 400 pulse with the scales: (a) 100 nm, (b) 500 nm

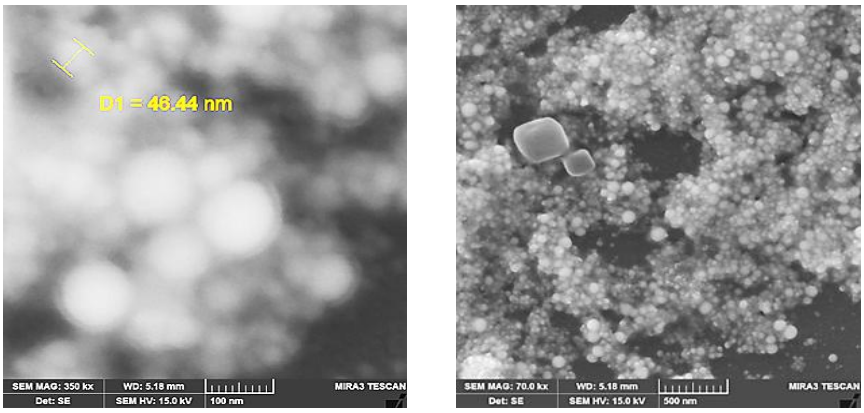

(a) (b)

Figure 14. FESEM images of AuNPs synthesized at 355 nm, 500 pulse with the scales: (a) 100 nm, (b) 500 nm

Figures 15, 16, & 17 show the results of EDX analysis of the prepared AuNPs at wavelengths (1064, 532, and 355 nm) respectively, which is useful in knowing the proportions of the chemical elements present. It turned out that the samples are composed of AuNPs in large, dominant proportions, which indicates the purity of the preparation technique used to obtain these nanoparticles. Additional peaks are observed in the EDX spectra, and the reasons back to technical or chemical aspect . This due to the presence of impurities on the surface of the sample or inside the instrument chamber, such as carbon or oxygen, or these peaks may result from the interaction of electrons with the sample carrier, such as copper or aluminum [52].

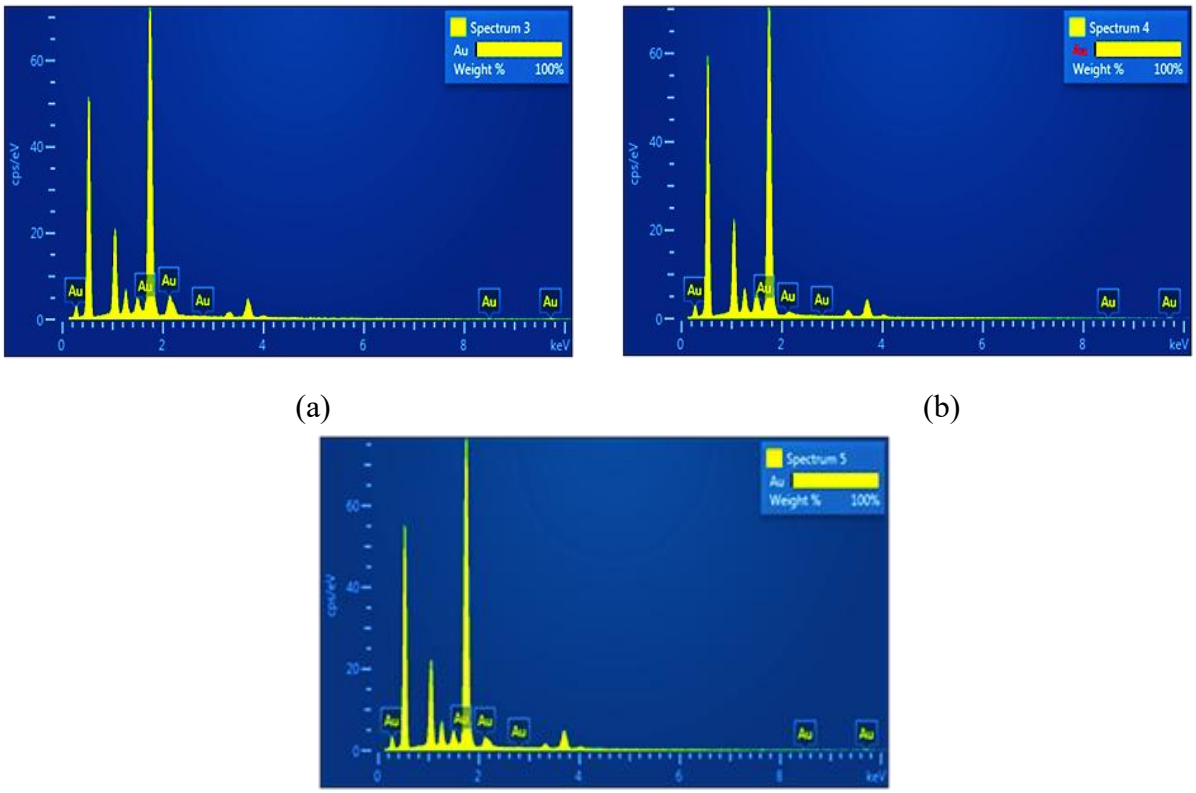

(a) (b)

(c)

Figure 15. EDX analysis of AuNPs synthesized at 1064 nm: (a) 300 pulse, (b) 400 pulse, (c) 500 pulse

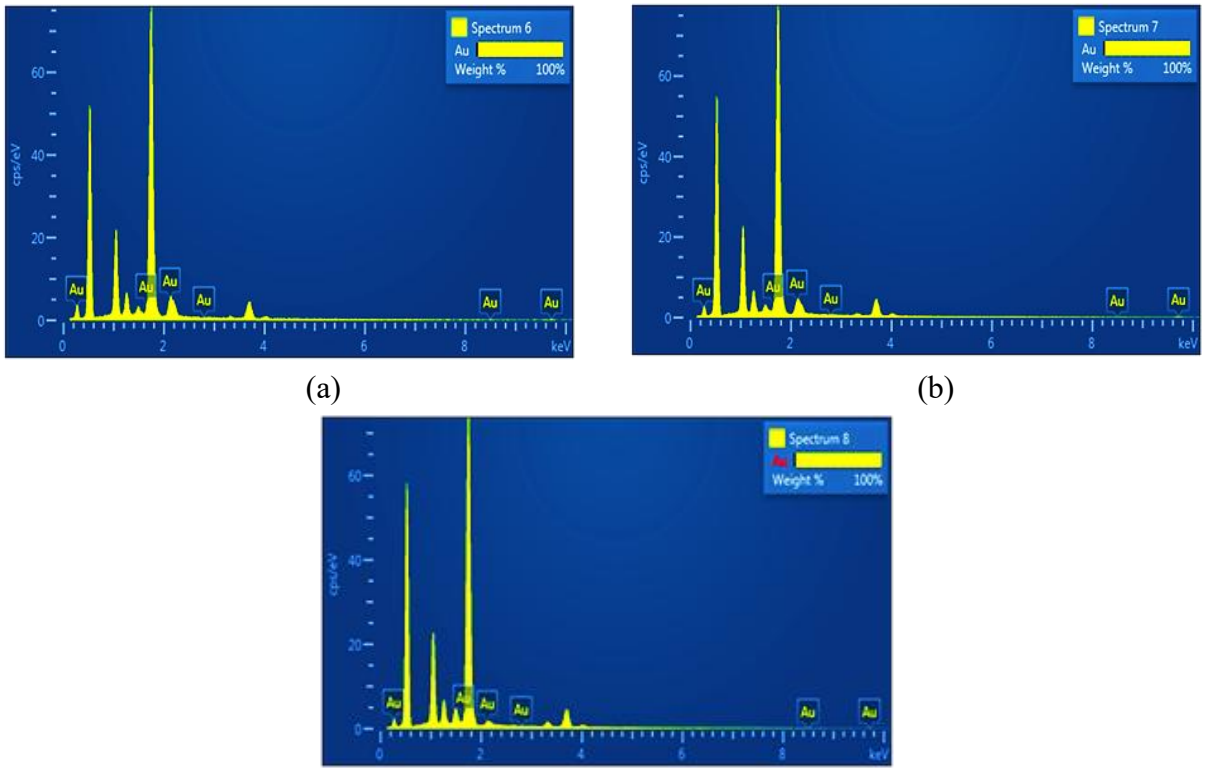

(a) (b)

(c)

Figure 16. EDX analysis of AuNPs synthesized at 532 nm: (a) 300 pulse, (b) 400 pulse, (c) 500 pulse

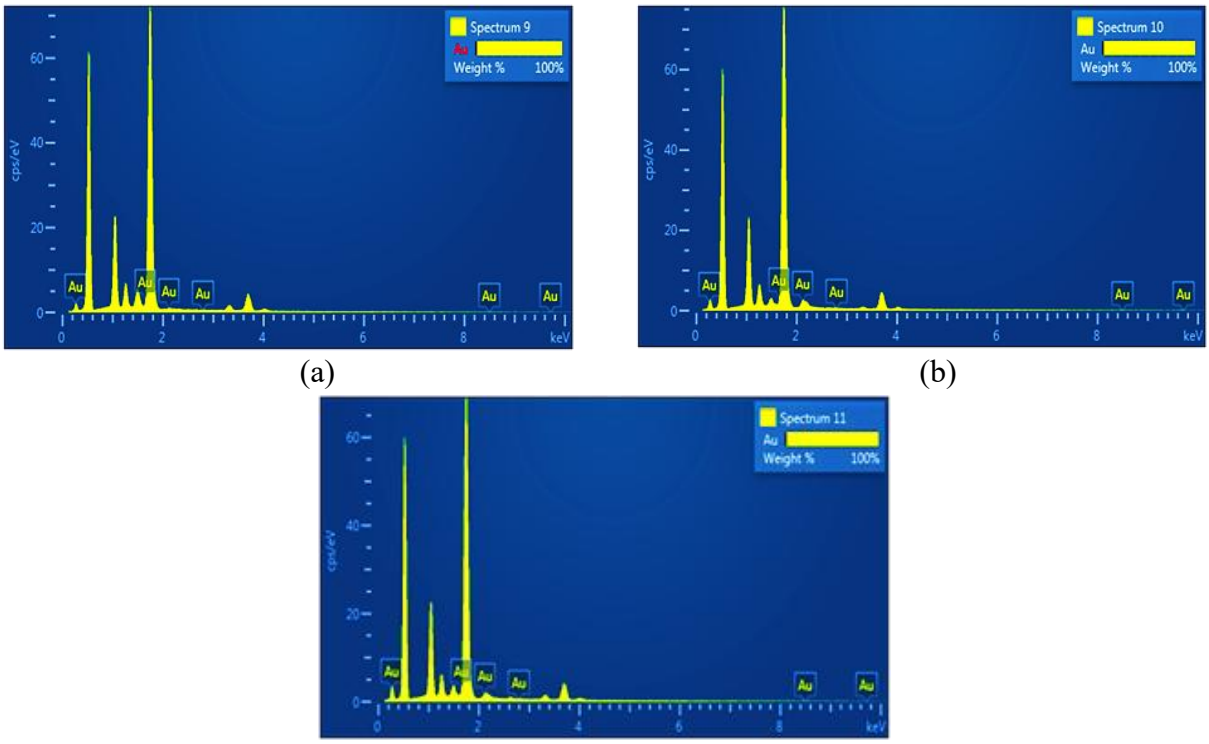

(a) (b)

(c)

Figure 17. EDX analysis of AuNPs synthesized at 355 nm: (a) 300 pulse, (b) 400 pulse, (c) 500 pulse

The results of the optical and structural properties analysis of the synthesized AuNPs show that the most suitable wavelength for their preparation under the current working conditions is (532 nm) compared to the two wavelengths (1064 and 355 nm), as the absorption spectrum of the NPs synthesized with this combination gave the highest peak and good width in comparison due to the regularity of the size distribution. Also, the XRD pattern showed that the size average decreased regularly with increasing the number of laser pulses. Additionally, from the surface morphology, it was found that the NPs prepared with the wavelength (532 nm) were regular with smaller diameter averages and a spherical shape, which allows a higher interaction area for various potential applications, this is agree with the previous studies [53, 54].

4. Conclusions

In this study, AuNPs have been synthesized by PLAL at different ablation wavelengths and pulse numbers. The presented NPs had an average crystallite size range (9 - 15 nm), and Composed in a different shape as some samples were elliptical and some were spherical, and this depends on the preparation conditions and the resulting concentrations which in turn depend on number of laser pulses and the wavelengths and their effect on the pulse energy. The Au nano-colloidal solutions appear reddish-pink and present an SPR around (527 nm). It turns out that the most appropriate wavelength for their preparation under the current working conditions is (532 nm) compared to the two wavelengths (1064 and 355 nm), as the crystallite size was smaller and the concentration of nanoparticles was higher, in addition to the high intensity of their absorption, where there is stable and high laser absorption at this wavelength by AuNPs. Based on these results, it is possible to produce AuNPs through a simple and low-cost method that can be used in a variety of potential applications.

References

[1] K. Ali, R. A. Khamis, and R. B. Rashid, "Preparation of Au-Ag Composite Nanoparticles by Pulsed Laser Ablation in Water for Controlling of AIP Enzyme Activity in Human Blood," Journal of the College of Basic Education, vol. 25, no. 103, pp. 23–36, 2019. https://doi.org/10.35950/cbej.v25i103.4544

[2] M. Lévy, D. Villa, G. Laurens, V. Blanchet, J. Bozek, J. Gaudin, E. Lamour, S. Macé, P. Mignon, A. R. Milosavljević, C. Nicolas, M. Patanen, C. Prigent, E. Robert, S. Steydli, M. Trassinelli, D. Vernhet, O. Veteläinen, and D. Amans, "Surface Chemistry of Gold Nanoparticles Produced by Laser Ablation in Pure and Saline Water," Langmuir, vol. 37, no. 19, pp. 5783–5794, 2021. https://doi.org/10.1021/acs.langmuir.1c00092

[3] S. R. Alizadeh, H. N. Seyghalan, Z. Hashemi, and M. A. Ebrahimzadeh, "Scrophularia Striata Extract Mediated Synthesis of Gold Nanoparticles; Their Antibacterial, Antileishmanial, Antioxidant, and Photocatalytic Activities," Inorganic Chemistry Communications, vol. 156, pp. 111138, 2023. https://doi.org/10.1016/j.inoche.2023.111138

[4] D. H. Al-Obaidi, O. A. Mahmood, A. A. Habeeb, and M. Z. Abdullah, "Preparation and Investigation of Gold Nanoparticles by the Technique of Laser Ablation for Biological Application," International Journal of Nanoelectronics and Materials, vol. 15, no. 3, pp. 269–280, 2022. https://ijneam.unimap.edu.my/index.php/vol-15-no-3-july-2022

[5] S. Jasim, K. A. Aadim, and S. N. Rashid, "Optical and Structural Properties of Cobalt Nanoparticles Synthesized by Laser Ablation," Iraqi Journal of Science, vol. 63, no. 10, pp. 4292–4304, 2022. https://doi.org/10.24996/ijs.2022.63.10.16

[6] M. Sajid and J. P. Wasylka, "Nanoparticles: Synthesis, Characteristics, and Applications in Analytical and Other Sciences," Microchemical Journal, vol. 154, pp. 104623, 2020. https://doi.org/10.1016/j.microc.2020.104623

[7] P. İpek, M. F. Baran, A. Baran, A. Hatipoğlu, C. Keskin, M. Yildiztekin, S. Küçükaydin, H. Becerekli, K. Kurt, A. Eftekhari, I. Huseynova, R. Khalilov, and W. Cho, "Green Synthesis and Evaluation of Antipathogenic, Antioxidant, and Anticholinesterase Activities of Gold Nanoparticles (Au NPs) from Allium cepa L. Peel Aqueous Extract," Biomass Conversion and Biorefinery, vol. 14, no. 9, pp. 10661–10670, 2024. https://doi.org/10.1007/s13399-023-04362-y

[8] S. N. Rashid, T. Y. Sabrib, S. A. Mahdi, and A. S. Jasim, "One-Step Fabricate of Copper Nanoparticles Via Pulsed Laser Ablation in Liquid: Influence of Energies on Physical Characterization," Defect and Diffusion Forum, vol. 421, pp. 45–52, 2022. https://doi.org/10.4028/p-h83031

[9] M. A. Fadhil, Z. S. Mohammed, Z. Y. Hasan, G. Al-Dahash, and N. M. Obaid, "An Effective Way to Prevent the Aggregation of Nanoparticles Prepared by the Laser Ablation in Colloidal Solutions," Solid State Technology, vol. 63, no. 2, pp. 1477–1488, 2020. https://www.solidstatetechnology.us/index.php/JSST/article/view/2749

[10] A. Khumaeni, W. S. Budi, S. Avicenna, M. Muniroh, N. Kusumaningrum, O. Damayanti, and S. Fitria, "Gold and Silver Nanoparticles as Computed Tomograpgy (CT) Contrast Agents Produced by a Pulsed Laser Ablation Technique: Study In- vitro and In-vivo," Rasayan Journal of Chemistry, vol. 16, no. 1, pp. 502–508, 2023. https://doi.org/10.31788/RJC.2023.1618202

[11] F. Sahebi, M. Ranjbar, and M. T. Goodarzi, "Synthesis of Gold Nanoparticles by Pulsed Laser-Assisted Reduction of Aqueous Gold Precursor," Applied Physics A, vol. 125, no. 12, pp. 850, 2019. https://doi.org/10.1007/s00339-019-3138-z

[12] S. Hammami, N. M. Alabdallah, A. Al-jomaa, and M. Kamoun, "Gold Nanoparticles: Synthesis Properties and Applications," Journal of King Saud University - Science, vol. 33, no. 6, pp. 101560, 2021. https://doi.org/10.1016/j.jksus.2021.101560

[13] M. Mitra, "Applications and Properties of Gold Nanoparticles," Nanoparticles, vol. 1, no. 1, pp. 4, 2019. https://doi.org/10.35702/nano.10004

[14] S. Sargazi, U. Laraib, S. Er, A. Rahdar, M. Hassanisaadi, M. N. Zafar, A. M. D. Pascual, and M. Bilal, "Application of Green Gold Nanoparticles in Cancer Therapy and Diagnosis," Nanomaterials, vol. 12, no. 7, pp. 1102, 2022. https://doi.org/10.3390/nano12071102

[15] L. S. De Bortoli, C. R. Vanoni, C. L. Jost, D. Z. Mezalira, and M. C. Fredel, "Stable and Ligand-Free Gold Nanoparticles Produced by Laser Ablation as Efficient Electrocatalysts for Electrochemical Sensing of Dopamine," Journal of Electroanalytical Chemistry, vol. 947, pp. 117744, 2023. https://doi.org/10.1016/j.jelechem.2023.117744

[16] Q. Fu, Y. Xie, F. Gao, R. Singh, X. Zhou, B. Zhang, and S. Kumar, "Four-Core Fiber-Based Multi-Tapered WaveFlex Biosensor for Rapid Detection of Vibrio Parahaemolyticus Using Nanoparticles-Enhanced Probes," Optics Express, vol. 32, no. 15, pp. 25772–25788, 2024. https://doi.org/10.1364/OE.530225

[17] Q. Zhang, C. Gu, R. Singh, S. Jain, R. T. Chen, B. Zhang, and S. Kumar, "Hump-Shaped Seven-Core Fiber-Based WaveFlex Biosensor for Rapid Detection of Glyphosate Pesticides in Real Food Samples," Optics Express, vol. 32, no. 15, pp. 25789–25804, 2024. https://doi.org/10.1364/OE.530348

[18] M. Maciulevičius, A. Vinčiūnas, M. Brikas, A. Butsen, N. Tarasenka, N. Tarasenko, and G. Račiukaitis, "On-Line Characterization of Gold Nanoparticles Generated by Laser Ablation in Liquids," Physics Procedia, vol. 41, pp. 531–538, 2013. https://doi.org/10.1016/j.phpro.2013.03.112

[19] S. Shirotiya, B. Singh, and Chauhan, "Green Synthesis of Gold Nanoparticles and its Diverse Applications in Various Fields," Annals of Plant Sciences, vol. 6, pp. 1720–1725, 2018. https://doi.org/10.21746/aps.2017.6.11.0

[20] E. Ogwuche, E. E. Elemike, D. Oju, D. C. Onwudiwe, M. Singh, and B. H. Akpeji, "Synthesis, Characterization, Anticancer and Antimicrobial Potentials of Chrysothemis Pulchella Leaf Extract Mediated Gold Nanoparticles," Journal of Inorganic and Organometallic Polymers and Materials, vol. 34, no. 3, pp. 944–951, 2024. https://doi.org/10.1007/s10904-023-02817-3

[21] L. Sortino, M. Censabella, G. Munzi, S. Boninelli, V. Privitera, and F. Ruffino, "Laser-Based Synthesis of Au Nanoparticles for Optical Sensing of Glyphosate: A Preliminary Study," Micromachines, vol. 11, no. 11, pp. 989, 2020. https://doi.org/10.3390/mi11110989

[22] M. Ghdhaib and S. N. Rashid, "Characterization of Nickel Oxide Nanoparticles Prepared Via Pulsed Laser Ablation: Evaluation of the Influence of Laser Parameters," Journal of

University of Anbar for Pure Science, vol. 18, no. 2, pp. 203–212, 2024. https://doi.org/10.37652/juaps.2024.148124.1224

[23] N. M. A. Fadhil and F. M. Jasim, "Study of Optical and Structural Properties of Prepared Gold Nanoparticles by Pulse Laser Ablation Method," Journal of Education and Science, vol. 30, no. 4, pp. 69–82, 2021. https://doi.org/10.33899/edusj.2021.129702.1148

[24] A. Balachandran, S. P. Sreenilayam, K. Madanan, S. Thomas, and D. Brabazon, "Nanoparticle Production via Laser Ablation Synthesis in Solution Method and Printed Electronic Application - A Brief Review," Results in Engineering, vol. 13, pp. 100646, 2022. https://doi.org/10.1016/j.rineng.2022.100646

[25] Z. Jiang, L. Li, H. Huang, W. He, and W. Ming, "Progress in Laser Ablation and Biological Synthesis Processes: “Top-Down” and “Bottom-Up” Approaches for the Green Synthesis of Au/Ag Nanoparticles," International Journal of Molecular Sciences, vol. 23, no. 23, pp. 14658, 2024. https://doi.org/10.3390/ijms232314658

[26] N. A. Hussain, L. Y. Abbas, and L. A. Latif, "Preparation of Nickel Oxide Microparticles by Pulsed Laser Ablation and Application to Gas Sensors," Journal of Engineering and Technology, vol. 6, no. 6, pp. 1011–1018, 2021. https://doi.org/10.30684/etj.v39i6.1593

[27] G. Lanza, D. Betancourth, A. Avila, H. Riascos, and J. A. Perez, "Control of the Size Distribution of AuNPs for Colorimetric Sensing by Pulsed Laser Ablation in Liquids," Kuwait Journal of Science, vol. 52, no. 1, pp. 100294, 2025. https://doi.org/10.1016/j.kjs.2024.100294

[28] L. Gentile, H. Mateos, A. Mallardi, M. Dell’Aglio, A. De Giacomo, N. Cioffi, and G. Palazzo, "Gold Nanoparticles Obtained by ns-Pulsed Laser Ablation in Liquids (ns-PLAL) are Arranged in the Form of Fractal Clusters," Journal of Nanoparticle Research, vol. 23, no. 2, pp. 35, 2021. https://doi.org/10.1007/s11051-021-05140-5

[29] J. G. Walter, S. Petersen, F. Stahl, T. Scheper, and S. Barcikowski, "Laser Ablation-Based One-Step Generation and Bio-Functionalization of Gold Nanoparticles Conjugated with Aptamers," Journal of Nanobiotechnology, vol. 8, no. 1, pp. 21, 2010. https://doi.org/10.1186/1477-3155-8-21

[30] N. Hodgson, S. Heming, A. Steinkopff, H. Haloui, and T. S. Lee, "Ultrafast Laser Ablation at 1035 nm, 517 nm and 345 nm as a Function of Pulse Duration and Fluence," Lasers in Manufacturing Conference, pp. 1–11, 2019. https://docslib.org/doc/7034401/ultrafast-laser-ablation-at-1035-nm-517-nm-and-345-nm-as-a-function-of-pulse-duration-and-fluence

[31] H. Naser, H. M. Shanshool, and K. I. Imhan, "Parameters Affecting the Size of Gold Nanoparticles Prepared by Pulsed Laser Ablation in Liquid," Brazilian Journal of Physics, vol. 51, no. 3, pp. 878–898, 2021. https://doi.org/10.1007/s13538-021-00875-x

[32] J. P. Rodrigo, Y. Maio, N. Faure, E. Kachan, J. P. Colombier, and X. Sedao, "Influence of the Wavelength on Femtosecond Laser Ablation Thresholds and Incubation

Coefficients of Silicon and Germanium," Journal of Laser Micro/Nanoengineering, vol. 19, no. 3, pp. 179–184, 2024. https://hal.science/hal-04820821/

[33] A. Habieb, A. O. Soary, and K. A. Mmohammed, "Effect of Laser wavelength on the Fabrication of Gold Nanoparticles by Laser Ablation," IMPACT: International Journal of Research in Applied, Natural and Social Sciences, vol. 4, no. 4, pp. 125–130, 2016. https://paper.researchbib.com/view/paper/75343

[34] N. Jamaludin, K. T. Chaudhary, Z. Haider, M. Duralim, F. D. Ismail, M. S. Roslan, N. H. Amira, and J. Ali, "Effect of laser energy and wavelength on average size of gold nanoparticles synthesized by pulsed laser ablation in deionized water," Journal of Physics: Conference Series, vol. 1484, pp. 012029, 2020. https://doi.org/10.1088/1742-6596/1484/1/012029

[35] L. Rapp, S. Madden, J. Brand, K. Maximova, L. J. Walsh, H. Spallek, O. Zuaiter, A. Habeb, T. R. Hirst, and A. V. Rode, "Investigation of laser wavelength effect on the ablation of enamel and dentin using femtosecond laser pulses," Scientific Reports, vol. 13, pp. 20156, 2023. https://doi.org/10.1038/s41598-023-47551-5

[36] Y. Xu, L. Yang, J. Li, D. Zhou, Q. Li, W. Shi, and Y. Jin, "Effect of laser wavelength on ablation propulsion and plasma characteristics with acrylonitrile butadiene styrene target," Journal of Physics D: Applied Physics, vol. 57, pp. 445201, 2024. https://doi.org/10.1088/1361-6463/ad6877

[37] D. Zhang, Z. Li, and K. Sugioka, "Laser ablation in liquids for nanomaterial synthesis: diversities of targets and liquids," Journal of Physics: Photonics, vol. 3, pp. 042002, 2021. https://doi.org/10.1088/2515-7647/ac0bfd

[38] H. Imam, K. Elsayed, M. A. Ahmed, and R. Ramdan, "Effect of Experimental Parameters on the Fabrication of Gold Nanoparticles via Laser Ablation," Optics and Photonics Journal, vol. 2, pp. 73–84, 2012. https://doi.org/10.4236/opj.2012.22011

[39] N. L. LaHaye, S. S. Harilal, P. K. Diwakar, A. Hassanein, and P. Kulkarni, "The effect of ultrafast laser wavelength on ablation properties and implications on sample introduction in inductively coupled plasma mass spectrometry," Journal of Applied Physics, vol. 114, pp. 023103, 2013. https://doi.org/10.1063/1.4812491

[40] K. Zhang, D. S. Ivanov, R. A. Ganeev, G. S. Boltaev, P. S. Krishnendu, S. C. Singh, M. E. Garcia, I. N. Zavestovskaya, and Chunlei Guo, "Pulse Duration and Wavelength Effects of Laser Ablation on the Oxidation, Hydrolysis, and Aging of Aluminum Nanoparticles in Water," Nanomaterials, vol. 9, no. 5, pp. 767, 2019. https://doi.org/10.3390/nano9050767

[41] N. K. Abdalameer, N. F. Majeed, A. K. Buraihi, and S. H. Ali, "Optical nanoparticle synthesis: a comprehensive laser ablation review," Journal of Optics, vol. 53, 2024. https://doi.org/10.1007/s12596-024-02299-7

[42] Lovkush, C. R. Kant, and P. Arun, "Tunability of Surface Plasmon Resonance Peaks in CsI:Ag Films by Growth Conditions," Plasmonics, vol. 15, no. 3, pp. 735–741, 2020. https://doi.org/10.1007/s11468-019-01061-1

[43] H. Kaur, H. Kaur, and A. Sharma, "Study of SPR peak shifting of silver nanoparticles with change in surrounding medium," Materials Today: Proceedings, vol. 37, pp. 3574–3576, 2021. https://doi.org/10.1016/j.matpr.2020.09.584

[44] H. N. Samani, R. S. Razavi, and R. Mozaffarinia, "Investigating the effect of 532 nm and 1064 nm wavelengths and different liquid media on the qualities of silver nanoparticles yielded through laser ablation," Materials Chemistry and Physics, vol. 305, pp. 128001, 2023. https://doi.org/10.1016/j.matchemphys.2023.128001

[45] M. Rodio, A. Scarpellini, A. Diaspro, and R. Intartaglia, "Tailoring of size, emission and surface chemistry of germanium nanoparticles via liquid-phase picosecond laser ablation," Journal of Materials Chemistry C, vol. 5, no. 46, pp. 12264–12271, 2017. https://doi.org/10.1039/C7TC01992K

[46] S. Demirel, T. Öztaş, C. Kurşungöz, I. Yılmaz, and B. Ortaç, "Synthesis of blue-shifted luminescent colloidal GaN nanocrystals through femtosecond pulsed laser ablation in organic solution," Journal of Nanoparticle Research, vol. 18, no. 5, pp. 128, 2016. https://doi.org/10.1007/s11051-016-3440-z

[47] X. Ren, Y. Song, A. Liu, J. Zhang, P. Yang, J. Zhang, and M. An, "Experimental and theoretical studies of DMH as a complexing agent for a cyanide-free gold electroplating electrolyte," RSC Advances, vol. 5, no. 80, pp. 64997, 2015. https://doi.org/10.1039/c5ra13140e

[48] G. Yang, "Laser Ablation in Liquids: Principles and Applications in the Preparation of Nanomaterials," PAN Stanford Publishing, CRC Press, Taylor & Francis Group, U.S., 1st ed., 2012. https://www.routledge.com/Laser-Ablation-in-Liquids-Principles-and-Applications-in-the-Preparation-of-Nanomaterials/Yang/p/book/9789814310956

[49] M. J. Haider and M. S. Mahdi, "Effect of Laser Wavelengths on the Silver Nanoparticles Size Prepared by PLAL," Journal of Engineering and Technology, vol. 34, pp. 1324–1334, 2016. https://doi.org/10.30684/etj.34.7A.6

[50] T. Patil, R. Gambhir, A. Vibhute, and A. P. Tiwari, "Gold Nanoparticles: Synthesis Methods, Functionalization and Biological Applications," Journal of Cluster Science, vol. 34, no. 2, pp. 705–725, 2023. https://doi.org/10.1007/s10876-022-02287-6

[51] J. Georgeous, N. AlSawaftah, W. H. Abuwatfa, and G. A. Husseini, "Review of Gold Nanoparticles: Synthesis, Properties, Shapes, Cellular Uptake, Targeting, Release Mechanisms and Applications in Drug Delivery and Therapy," Pharmaceutics, vol. 16, no. 10, pp. 1332, 2024. https://doi.org/10.3390/pharmaceutics16101332

[52] J. I. Goldstein, D. E. Newbury, J. R. Michael, N. W. M. Ritchie, J. H. J. Scott, and D. C. Joy, "Energy Dispersive X-ray Spectrometry: Physical Principles and User-Selected

Parameters," Scanning Electron Microscopy and X-Ray Microanalysis, Springer, New York, NY, pp. 209–234, 2018. https://doi.org/10.1007/978-1-4939-6676-9_16

[53] J. Khamees and O. Gençyılmaz, "Comparison of alternative gold nanoparticles (AuNPs) produced by laser ablation technique for photothermal therapy applications," Journal of Optics, vol. 54, no. 4, pp. 2419–2431, 2025. https://doi.org/10.1007/s12596-024-01962-3

[54] M. R. Maina, Y. Okamoto, K. Hamada, A. Okada, S. Nakashiba, and N. Nishi, "Effects of Superposition of 532 nm and 1064 nm Wavelengths in Copper Micro-Welding by Pulsed Nd:YAG Laser," Journal of Materials Processing Technology, vol. 299, pp. 117388, 2022. https://doi.org/10.1016/j.jmatprotec.2021.117388

تحضير جسيمات الذهب النانوية باستخدام تقنية الاستئصال بالليزر: تأثير الأطوال الموجية وعدد النبضات

مها محمد ابراهيم و فالح لفته مطر و سحر ناجي رشيد

قسم الفيزياء, كلية العلوم, جامعة تكريت, صلاح الدين، العراق.

المستخلص

إن إمكانية إنتاج تراكيب نانوية نقية وخالية من الشوائب تجعل من الاستئصال بالليزر في السوائل تقنيةً مثيرةً للاهتمام لإنتاج التراكيب النانوية. يتميز هذا النهج الفيزيائي بسهولته وأمانه واقتصاديته وسرعته مقارنةً بتقنيات التحضير البايولوجية والكيميائية. في هذه الدراسة، طُبقت هذه التقنية لتحضير جسيمات الذهب النانوية باستخدام ليزر Nd: YAG النبضي ذي طاقة ثابتة ومعدل تكرار ثابت. تم تغيير الأطوال الموجية، واستُخدمت ثلاثة توافقيات (1064، 532، و355 نانومتر). أُجري الاستئصال باستخدام أعداد نبضات مختلفة (300، 400، و500 نبضة) لكل توافقية، واستُخدم الماء منزوع الأيونات كوسط سائل، مما نتج عنه محلول غرواني ذو لون وردي محمر يحتوي على جسيمات نانوية من الذهب. تم توصيف الجسيمات النانوية الناتجة تركيبيًا وبصريًا. بشكل عام، تراوح متوسط أحجام البلورات النانوية الناتجة بين 9 و15 نانومترًا، وظهرت بأشكال مختلفة، حيث كانت بعض العينات بيضاوية وبعضها كروية، وذلك تبعًا للحجم والتركيز الناتجين عن تغيير معايير الاستئصال، حيث تراوح متوسط أقطارها بين 11 و46 نانومترًا. وقد أثرت هذه المعايير أيضًا على عرض وارتفاع ذروة امتصاص الجسيمات النانوية، والتي تمثل رنين البلازمون السطحي. وبناءً على ذلك، وُجد أن الطول الموجي الأمثل للتحضير في هذه الدراسة هو 532 نانومترًا.

الكلمات المفتاحية: جسيمات الذهب النانوية، الغرويات، معلمات الليزر، الاستئصال بالليزر النبضي في السائل، رنين البلازمون السطحي.